DYNAMICS OF MARINE PIPELINES - A NONLINEAR ANALYSIS

Leandro Ribeiro dos Santos
Federal University of Rio de Janeiro, PEM/COPPE. P.O.Box 68503, 21945-970, Rio de Janeiro, RJ, Brazil.
leandro@mecsol.ufrj.br

Fernando Alves Rochinha
Federal University of Rio de Janeiro, PEM/COPPE. P.O.Box 68503, 21945-970, Rio de Janeiro, RJ, Brazil.
faro@serv.com.ufrj.br

Abstract. The dynamics of marine pipelines is becoming increasingly important in engineering. These systems including flexible risers, umbilicals, synthetic ropes, tethers and towed pipelines are used in the oil exploitation in deep waters and undergo large deformations, which requires nonlinear analysis. All those systems are usually modeled as one-dimensional structures, often referred to as rods. In the present work a Cosserat continuum theory is adopted, in which the geometry of the rod is described by a smooth mapping defining the spatial position of the line of centroids and an orthonormal frame, which defines the relative orientation of the cross-section attached to each point of the curve. In order to solve the nonlinear evolution equations resulting from the modeling, a time-stepping numerical algorithm, which achieves stable solutions combined with high precision, was developed. This time-stepping algorithm preserves exactly fundamental constants of the motion, namely the total linear and total angular momentums and, for the Hamiltonian case, the total energy. In the literature, numerical schemes capable of preserving those quantities are known as conserving algorithms. Three main reasons can be pointed out to motivate the use of such algorithms: the role played by those quantities in the physical and mathematical context; the enhanced numerical capabilities of those algorithms and, finally, the conserved quantities often represent qualitative features of the long term dynamics. The objective of the present work is to use this numerical framework to the simulation of the nonlinear dynamics of rods to analyze the dynamical behavior of marine pipelines. In particular, in order to check the performance of the proposed approach, some examples of cables (starting from different static equilibrium states) being excited dynamically are considered. The results show the stability of the algorithm and accuracy when testing it for different boundary conditions, loading histories and finite element meshes.

Keywords: cables, dynamics, rods, nonlinear

1. Introduction

The design of many structural systems, like cables, spacecraft antennae, helicopter rotor blades, robot arms and other systems that perform complex motions, requires an accurate description of the dynamical behavior. In the above examples, the involved structures can be thought as one-dimensional rods.Indeed, the existing literature over these topics is very vast and includes a variety of formulations from different perspectives. A central issue, from a numerical analysis perspective, concerns the specific choice of the parametrization used in the mathematical description of large rotations. A particular field of great engineering interest is the oil exploitation in deep waters, in which marine systems including flexible risers, umbilicals, synthetic ropes, tethers and towed pipelines undergo large deformations which requires nonlinear analysis. In the present work, the dynamics of these structures is referred directly to the inertial frame, such that the motion due to rigid rotations of the cable is not distinguished from that due to deformations. In addition, the structure of inertia operator is similar to that arising from rigid body mechanics. The inherent nonlinear character of the problem lies in the stiffness operator. It has been shown by several researchers, in the recent past, that care has to be taken with the use of time stepping schemes for the solution of nonlinear dynamic equations. One of the most commonly employed time-stepping method in structural dynamics, applied in both linear and nonlinear problems, is the Newmark family of algorithms (Hughes, 1987), which includes the trapezoidal rule as a special case. The objective of the present work is to use a numerical algorithm dedicated to the simulation of the nonlinear dynamics of rods (Rochinha, 1990) and (Dolinski, 1996) to simulate the dynamical behavior of marine pipelines. This time-stepping algorithm preserves exactly fundamental constants of the motion, namely the total linear and total angular momentums and, for the Hamiltonian case, the total energy. In the literature, numerical schemes capable of preserving those quantities are known as conserving algorithms. Three main reasons can be pointed out to motivate the use of such algorithms: the role played by those quantities in the physical and mathematical context; the enhanced numerical capabilities of those algorithms and, finally, the conserved quantities often represent qualitative features of the long term dynamics. The nonlinear system of partial differential equations governing the dynamic of the cables is cast in a variational formulation by using an extended form of the Hamilton's principle introduced in (Bailey, 1987). This variational formulation allows the use of the Finite Element Method for obtaining a spatial discretization of the problem. The resulting nonlinear ordinary differential equation is solved by the proposed implicit time integration scheme. Finally, some numerical examples, which include cables undergoing large overall motions, are presented to illustrate that this new formulation achieves precision and stability in the nonlinear

range.

2. Nonlinear dynamics of rods

A brief summary of the equations governing the nonlinear dynamics of rods undergoing finite extension, shear, twist and bending is presented. Only aspects of the theory relevant to the subsequent algorithmic development are presented. The geometry of the cable is described by a mapping defining the spatial position of the line of centroids and the orientation of an orthonormal frame associated to the cross-section attached to each point of the line as shown in Fig. 1. The basic kinematic assumption is that cross-sections undergo rigid body motion. Accordingly,

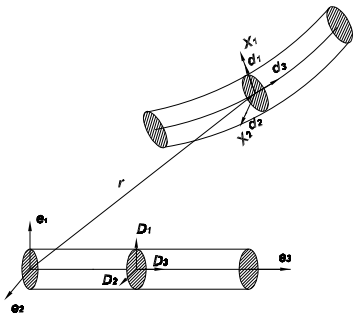

Figure 1. Geometric description of cables deformation

$$\chi(S,t) = \mathbf{r}(S,t) + \mathbf{X}_1\ \mathbf{d_1}(S,t) + \mathbf{X}_2\ \mathbf{d_2}(S,t) \tag{1}$$

where $\mathbf{r}(S,t)$ defines the cartesian position of the centerline which is parameterized by S (arc-length in the undeformed configuration). $\mathbf{d}_i(S,t)$ are orthonormal vector fields called directors (Antman and Kenney 1981), defined in each point of line c, which provide the cross-section orientation in current configuration. It is also introduced the frame e_i representing an inertial basis in the three-dimensional Euclidean space $\Re^3$. From Eq. (1), a configuration of the rod is completely described by the pair

$$\Phi = (\mathbf{r}, \mathbf{d_i}) \ \in \ K = V \text{ x } K \quad (i = 1,2,3) \tag{2}$$

with

$V = \{\mathbf{r} : [0, L] \rightarrow R^3 \ \text{ and appropriate boundary conditions}\}$

and the nonlinear manifold K defined by

$K = \{(\mathbf{d_1}, \mathbf{d_2}, \mathbf{d_3}) : [0, L] \rightarrow R^9 \ / \ \mathbf{d_i}.\mathbf{d_j} = \delta_{ij} \ \ (i, j = 1, 2, 3) \text{ and appropriate boundary conditions}\}$

where δ_{ij} is the delta of kronecker and 0 and L represent the boundary points of the rod.
Consequently, one refers to K as the abstract configuration manifold of the rod.
The strain components in this modeling are defined using the vector field $\mathbf{u}(S,t)$ obtained as

$$\mathbf{d'}_{\mathrm{k}}(\mathrm{S},\mathrm{t}) = \mathbf{u}(\mathrm{S},\mathrm{t}) \wedge \mathbf{d}_{\mathrm{k}}(\mathrm{S},\mathrm{t}) \tag{3}$$

where $()'$ denotes the partial derivative with respect to S, and $\wedge$ is the ordinary vectorial product. Thus, the following strain measures are considered

$$\bar{\mathbf{u}}_{\mathrm{k}}(\mathrm{S},\mathrm{t}) = \mathbf{u}_{\mathrm{k}}(\mathrm{S},\mathrm{t}) - \mathbf{U}_{\mathrm{k}}(\mathrm{S},0) \quad (\mathrm{k} = 1,3) \tag{4}$$

where the $\mathbf{U}_k$ are calculated through Eq. (3) applied to the directors in the reference configuration. The components $\bar{\mathbf{u}}_k (k = 1, 2)$ and $\bar{\mathbf{u}}_3$ represent, respectively, flexion and torsion strain measures. Note that the strain vector is unaltered by superposed rigid motions and vanish at the reference configuration. It is not required that the rod's cross-section remains orthogonal to the neutral axis (curve c), or that neutral axis should be inextensible as well.

Associated with the motion, the velocities and accelerations fields are introduced through the standard expressions

$$\mathbf{v} = \dot{\mathbf{r}}; \mathbf{a} = \ddot{\mathbf{r}}; \dot{\mathbf{d}}_{\mathrm{k}}; \ddot{\mathbf{d}}_{\mathrm{k}} \tag{5}$$

where $\dot{()}$ stands for the time derivative.The first two fields are,respectively, the translational velocity and the translational acceleration. The others describe the velocity and acceleration of the angular motion and are related to angular velocity and angular acceleration of the cross-section by means of

$$\dot{\mathbf{d}}_{\mathrm{k}} = \omega \wedge \mathbf{d}_{\mathrm{k}}; \ddot{\mathbf{d}}_{\mathrm{k}} = \alpha \wedge \mathbf{d}_{\mathrm{k}} + \omega \wedge (\omega \wedge \mathbf{d}_{\mathrm{k}}) \tag{6}$$

2.1 Local form of the momentum balance equations

The nonlinear system of partial differential equations governing the motion of the rod is constituted by the balance of linear and angular momentum (Antman and Kenney, 1981), e.g:

$$\mathbf{n}'+\overline{\mathbf{n}} = \overline{\rho}\mathbf{a} \tag{7}$$

$$\mathbf{m}' + \mathbf{r}' \wedge \mathbf{n}+\overline{\mathbf{m}} = \mathrm{I}^{\rho}_{22}(\mathbf{d}_1 \wedge \ddot{\mathbf{d}}_1) + \mathrm{I}^{\rho}_{11}(\mathbf{d}_2 \wedge \ddot{\mathbf{d}}_2) \tag{8}$$

where $\mathbf{n}$ and $\mathbf{m}$ denote the contact resultant force and contact resultant couple per unit of reference arc-length, $\overline{\mathbf{n}}$ and $\overline{\mathbf{m}}$ are prescribed body forces and body couples per unit of arc-length acting on the rod, $\overline{\rho}$ is the mass-density function per unit of reference arc-length which can be interpreted as the average of the three-dimensional density function, ρ , over the cross section of the rod and I^{ρ} is the inertial moment of the mass ($I^{\rho}_{11} = \int_A \rho X_2^2 dA$ and $I^{\rho}_{22} = \int_A \rho X_1^2 dA$). Here, A denotes the area of the cross-section.

2.2 Variational principle

In the present section, the system of differential equations formed by Eqs. (7) and (8) is cast in a variational formulation with the aid of an extended version of the Hamilton's principle introduced by (Bayley, 1987). This version differs from the classical least action variational principle by the inclusion of an end-point term, yielding

$$\delta \int_{\mathrm{t_1}}^{\mathrm{t_2}} [\mathrm{J_{kin}}(\phi,\mathrm{t}) - \mathrm{J_{pot}}(\phi,\mathrm{t})]\mathrm{dt} - \tfrac{\partial \mathrm{J_{kin}}}{\partial \mathbf{r}}\ \mathbf{p}|_{\mathrm{t_1}}^{\mathrm{t_2}} - \sum_{\mathrm{i}=1}^{3} \tfrac{\partial \mathrm{J_{kin}}}{\partial \mathbf{d_i}}\ \mathbf{g_i}|_{\mathrm{t_1}}^{\mathrm{t_2}} = 0; \forall \phi = (\mathbf{r}, \mathbf{d_k}) \in \mathrm{K} \tag{9}$$

where J_{kin} is the kinetic energy of the system and J_{pot} is the potential energy, which includes both strain energy and the potential of any conservative external forces; like, for instance, forces which are independent of the deformation and motion of the rod. Here δ denotes the variational operator. Thus, the expression of the variation of kinetic energy is given by

$$\delta \mathrm{J_{kin}} = -\int_{\mathrm{t_1}}^{\mathrm{t_2}} \left(\int_0^{\mathrm{L}} (\overline{\rho}\mathbf{a}.\mathbf{p} + \mathrm{I}^{\rho}_{22}\ddot{\mathbf{d}}_1.\mathbf{g}_1 + \mathrm{I}^{\rho}_{11}\ddot{\mathbf{d}}_2.\mathbf{g}_2)\mathrm{dS} \right) \mathrm{dt}; \forall \eta = (\mathbf{p}, \mathbf{g_i}) \in \mathrm{dK} \tag{10}$$

where dK is the tangent space at K, defined by

$$\mathrm{dK} = \{(\mathbf{p}, \mathbf{g_i}) : [0, \mathrm{L}]\mathrm{x}[\mathrm{t_1}, \mathrm{t_2}] \rightarrow \Re^3 \mathrm{x} \Re^9 \,|\mathbf{g_i} = \mathbf{U} \wedge \mathbf{d_i} (\mathbf{U} \in \Re^3)\ \} \tag{11}$$

and represents the set of admissible variations.

In equation above, it is assumed without lost of generality, that directors are collinear to the principal axis of inertia and that the curve c is coincident with the line of centroids. One may observes that in this case the translational inertia is completely decoupled from the rotatory inertia, resulting in a similar form to the one of the rigid body dynamics. The expression of the variation of total potential energy is so given by

$$\delta \mathrm{J_{pot}} = \int_{\mathrm{t_1}}^{\mathrm{t_2}} \left\{ \int_0^{\mathrm{L}} \sum_{\mathrm{i}=1}^{3} \tfrac{\partial \Psi}{\partial \mathbf{d_i}}.\mathbf{g_i}\mathrm{dS} - \int_0^{\mathrm{L}} \overline{\mathbf{n}}.\mathbf{p} dS - \sum_{\alpha=1}^{2} \int_0^{\mathrm{L}} \overline{\mathbf{n}}_\alpha \mathbf{g}_\alpha \mathrm{dS} + \right.$$

$$\left. + \int_0^{\mathrm{L}} \mathrm{R}(\mathbf{r}^{'} - \mathbf{d}_3).(\mathbf{p}' - \mathbf{g}_3)\mathrm{dS} + \sum_{\mathrm{i}=1}^{3}\sum_{\mathrm{j}=\mathrm{i}}^{3} \int_0^{\mathrm{L}} \lambda_{\mathrm{ij}}(\mathbf{g_i}.\mathbf{d_j} + \mathbf{g_j}.\mathbf{d_i})\mathrm{dS} \right\} \mathrm{dt}; \forall (\mathbf{p}, \mathbf{g_i}) \in \mathrm{dK} \tag{12}$$

where Ψ is the elastic energy density, has the following form

$$\Psi(\mathrm{S}, \overline{\mathrm{u}}, \overline{\mathrm{w}}) = \tfrac{1}{2}(\mathrm{EI_1}\overline{\mathrm{u}}_1^2 + \mathrm{EI_2}\overline{\mathrm{u}}_2^2 + \mathrm{GJ}\overline{\mathrm{u}}_3^2)$$

and λ_{ij} are the lagrange multipliers associated to the orthonormality constraint. In Eq. (12), the effects of shear and extension are introduced via a penalty method. Here, the parameter of penalty R is adopted equal the axial stiffness of the rod. Besides, E and G are interpreted as the Young's modulus and the shear modulus, I_1 and I_2 are the principal moments of inertias and J is the torsional modulus.

2.3 Hydrodynamic loads

In this work, the marine current force acting in the cable is computed using Morison's Formula, so that the transversal load vectors due to the fluid-structure interaction are written as

(1) Transverse drag force

$$\mathbf{f}_{Dn} = \frac{1}{2}\rho_W D C_{Dn} \dot{\mathbf{v}}_{rn} |\dot{\mathbf{v}}_{rn}| \tag{13}$$

(2) Skin friction or tangential drag force

$$\mathbf{f}_{Dt} = \frac{1}{2}\rho_W D C_{Dt} \dot{\mathbf{v}}_{rt} |\dot{\mathbf{v}}_{rt}| \tag{14}$$

where

$$\mathbf{v}_r = \mathbf{v}_c - \mathbf{v} \tag{15}$$

$$\mathbf{v}_{rn} = \mathbf{v}_r - \mathbf{v}_{rt} = \mathbf{v}_r - (\mathbf{v}_r.\mathbf{d}_3)\mathbf{d}_3 \tag{16}$$

$$\mathbf{v}_{rt} = (\mathbf{v}_r.\mathbf{d}_3)\mathbf{d}_3 \tag{17}$$

In the above expressions $\mathbf{v}_r$ is the relative fluid velocity, $\mathbf{v}_c$ is the current velocity, $\mathbf{v}_{rn}$ is the component of $\mathbf{v}_r$ acting normally to the pipe, $\mathbf{v}_{rt}$ is the tangential component of and $|\mathbf{v}_{rn}| = (\mathbf{v}_{rn}^T \mathbf{v}_{rn})^{1/2}$ is the magnitude of $\mathbf{v}_{rn}$. In Eqs. (13) and (14), D is the effective drag (hydrodynamic) diameter of pipe, C_{Dn} is the transverse (normal) drag coefficient and C_{Dt} is the tangential drag coefficient. Both these coefficients are obtained from experiments and are functions of the Reynolds number. It is noted that tangential drag coefficient normally has a small value compared to the normal drag coefficient and is often neglected.

The total hydrodynamic load acting to the pipe is the vectorial sum of Eqs. (13) and (14).It is important to notice here that these drag loads are of the non-conservative type because they have a dependency on the configurations assumed by the structure.

2.4 Numerical Approximation

The numerical treatment of the variational Eq. (9) is based on a semi-discrete approach involving the spatial discretization through the Finite Element Method and the temporal discretization via the time stepping procedure introduced in (Dolinski, 1996). The resulting nonlinear algebraic system is solved employing the Newton-Raphson method. The novelty of the proposed approach lies in the treatment of the rotational component of the movement, namely the evolution of the directors.

The functions associated to the translational motion $(\mathbf{r}, \mathbf{v})$ are discretized by cubic Hermitian finite elements and those associated to the rotational movement $(\mathbf{d}_i, \dot{\mathbf{d}}_i)$ by quadratic Lagrangian functions. Details of the implementation of the finite element discretization can be found in (Rochinha , 1990), where the static case is addressed.

A numerical evolution scheme consists in given a configuration $\Phi_n := (\mathbf{r}^n, \mathbf{d}_i^n) \in K$ and its associated velocities $(\mathbf{v}^n, \dot{\mathbf{d}}_i^n)$, to obtain the updated configuration $\Phi_{n+1} := (\mathbf{r}^{n+1}, \mathbf{d}_i^{n+1}) \in K$ and the associated velocities $(\mathbf{v}^{n+1}, \dot{\mathbf{d}}_i^{n+1})$, satisfying the governing equations.

Moreover, let $[t_n, t_{n+1}]$ be a typical interval $[0, \bar{t}] = U_{n=0}^{N}[t_n, t_{n+1}]$ and let $\Delta t = t_{n+1} - t_n$ be the time step interval. The main steps of the proposed algorithm are summarized below.

- Admit the initial configuration

position: $\Phi_{(0)}^n := (\mathbf{r}_{(0)}^n, \mathbf{d}_{i(0)}^n) \in K$
velocities: $(\mathbf{v}_{(0)}^n, \dot{\mathbf{d}}_{\mathbf{i(0)}}^n)$

- Step 0: Define a predictor for the translational and rotational fields

• Translation

$\mathbf{r}^{n+1} = \mathbf{r}^n$
$\mathbf{v}^{n+1} = -\mathbf{v}^n$

• Rotation

$\mathbf{d}_i^{n+1} = \mathbf{d}_i^n$

$$\dot{\mathbf{d}}_{\mathbf{i}}^{n+1} = -\dot{\mathbf{d}}_{\mathbf{i}}^{n}$$

Here, the superscripts n and n+1 denotes the temporal discrete approximation of a time-varying quantity at time t_n and t_{n+1} respectively.

- Step 1: Compute the lagrange multipliers $\lambda_{ik(j)}^{n+\frac{1}{2}}$ by solving

$$L(\phi_{(j),\eta}^{n+1}) = \int_0^L \bar{\rho}\,\frac{\mathbf{v}^{n+1}-\mathbf{v}^n}{\Delta t}\cdot\mathbf{p}dS + \int_0^L I_{22}^{\rho}\frac{\dot{\mathbf{d}}_1^{n+1}\cdot\mathbf{g}_1^{n+1}-\dot{\mathbf{d}}_1^{n}\cdot\mathbf{g}_1^{n}}{\Delta t}\,dS + \int_0^L I_{11}^{\rho}\frac{\dot{\mathbf{d}}_2^{n+1}\cdot\mathbf{g}_2^{n+1}-\dot{\mathbf{d}}_2^{n}\cdot\mathbf{g}_2^{n}}{\Delta t}\,dS +$$

$$+\int_0^L EI_1(\mathbf{d}_3^{'n+\frac{1}{2}}\cdot\mathbf{g}_2^{n+\frac{1}{2}}+\mathbf{g}_3^{'n+\frac{1}{2}}\cdot\mathbf{d}_2^{n+\frac{1}{2}})dS + \int_0^L EI_2(\mathbf{d}_1^{'n+\frac{1}{2}}\cdot\mathbf{g}_3^{n+\frac{1}{2}}+\mathbf{g}_1^{'n+\frac{1}{2}}\cdot\mathbf{d}_3^{n+\frac{1}{2}})dS +$$

$$+\int_0^L GJ(\mathbf{d}_2^{'n+\frac{1}{2}}\cdot\mathbf{g}_1^{n+\frac{1}{2}}+\mathbf{g}_2^{'n+\frac{1}{2}}\cdot\mathbf{d}_1^{n+\frac{1}{2}})dS + \int_0^L R(\mathbf{r}'-\mathbf{d_3})^{n+\frac{1}{2}}\cdot(\mathbf{p}'-\mathbf{g}_3^{n+\frac{1}{2}})dS +$$

$$+\sum_{i=1}^{3}\sum_{j=1}^{3}\int_0^L \lambda_{ik}^{n+\frac{1}{2}}(\mathbf{d_i}\mathbf{g_k}+\mathbf{d_k}\mathbf{g_i})^{n+\frac{1}{2}}dS - \int_0^L \mathbf{f}^{n+\frac{1}{2}}\cdot\mathbf{p}dS - \sum_{\alpha=1}^{2}\int_0^L \frac{\mathbf{f}^{n+1}\cdot\mathbf{g}_\alpha^{n+1}+\mathbf{f}^{n}\cdot\mathbf{g}_\alpha^{n}}{2}dS = 0$$

for a convenient choice of $\mathbf{g_i}$ and where the notation $()^{n+\frac{1}{2}} = \frac{()^n+()^{n+1}}{2}$

- Step 2: Compute the residual $R_{(j)}^{n+1}$ of the above equation and check the convergence
Computation of the $R_{(j)}^{n+1}$ by choosing $\mathbf{g}_i^{n+1} = \mathbf{U}\wedge\mathbf{d}_{\mathbf{i(j)}}^{\mathbf{n+1}}$ and $\mathbf{g}_i^{n+\frac{1}{2}} = \mathbf{U}\wedge(\frac{\mathbf{d}_i^{n+1}+\mathbf{d}_i^n}{2})$

Check for convergence: IF $\|R_{(j)}^{n+1}\| \leq$ tolerance then begin new time step ($n \rightarrow n+1$, go to step 0).

Else: continue

Here (j) denotes the iteration of the Newton-Raphson.

- Step 3: Compute tangent matrix

$$K_T = [\frac{\partial^2 L}{\partial(\mathbf{r}^{n+1},\mathbf{d}_i^{n+1})}(\mathbf{p},\mathbf{g_i})](\bar{\mathbf{p}},\bar{\mathbf{g}}_\mathbf{i})$$

$$\forall(\mathbf{p},\mathbf{g_i}) \in dK \; and \; \forall(\bar{\mathbf{p}},\bar{\mathbf{g}}_\mathbf{k}) \in dK$$

and solve the linear system $K_T(\bar{U},\bar{\mathbf{p}}) = R_{(j)}^{n+1}$

- Step 4: Update the configuration

• Translation

$$\mathbf{r}_{(j+1)}^{n+1} = \mathbf{r}_{(j)}^{n+1} + \mathbf{p}_{(j)}^{-n+1}$$

$$\mathbf{v}_{(j+1)}^{n+1} = \mathbf{v}_{(j)}^{n+1} + \tfrac{2}{\Delta t}\mathbf{p}_{(j)}^{-n+1}$$

• Rotation

$$\mathbf{d}_{i(j+1)}^{n+1} = Cay(\mathbf{d}_{i(j)}^{n+1} + \mathbf{g}_{i(j)}^{-n+1})$$

$$\dot{\mathbf{d}}_{i(j+1)}^{n+1} = (I+Q)^{-1}\{\tfrac{4}{\Delta t}(d_i^{n+1}-d_i^n) + (I+Q^T)\dot{\mathbf{d}}_i^n\}$$

where Cay denotes for the Cayley transform (Geradin, 1994) a mapping from R^3 to SO(3), the special group of rotations and $Q = (\mathbf{d}_{i(j)}^{n+1}\otimes\mathbf{d}_i^n)$.

- Step 5: Begin new iteration; $j \rightarrow j+1$ go to step 2.

2.5 Numerical Simulation

The numerical methodology presented in this work will now be used in typical situations involving the nonlinear dynamics of undersea cables.

Consider a cable, hanging from a floating system in one end and fixed in the other end. If l is the length of the cable, the coordinate of the point anchored in the floating system is $S = 0$ and $S = l$ being the coordinate of the other fixed end. In this work two cables with different material properties will be analyzed.

Given the static equilibrium states of the flexible cables depicted in Fig. 2 and 3, suppose that an harmonic motion $U(t) = U_0 sin(wt)$ in the vertical direction is imposed at the suspended end $S = 0$. This displacement is due to the platform motion. Physical and geometric cables characteristics used in the numerical analysis are presented in Tab. 1.

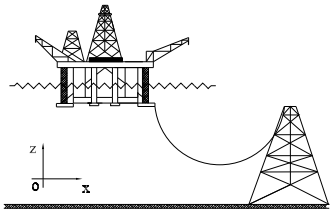

Figure 2. Catenary equilibrium shape.

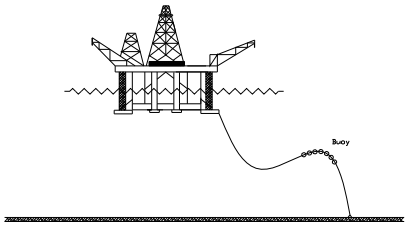

Figure 3. Lazy wave equilibrium shape.

Table 1. Material properties and hydrodynamic coeficients of the cables

Material properties	Cable of Fig. 2	Cable of Fig. 3
Weight in air (kg/m)	226.7	138.3
Outside diameter (m)	0.3172	0.332
Axial stiffness (N)	$7.96.10^8$	$4.58.10^8$
Bending stiffness (Nm^2)	$5.882.10^4$	$1.01.10^5$
Torsional stiffness (Nm^2/rad)	$9.25.10^6$	$5.7.10^6$
Hydrodynamic coefficients		
Normal drag coefficient	0.6	0.8
Tangential drag coefficient	0.05	0.05

It is importante to notice that in the finite element model representation and analysis the following cables characteristics have been considered:

(a) Fluid loading on the cables results from normal and tangential force components obtained from Morison's formula;

(b) In the numerical model proposed, the following loadings are included: gravitational, buoyancy, current and due to the platform's motion;

(c) The material properties of the cables, the current profile and phase and amplitude parameters of the platform's motion are typical in common operation conditions.

The 100m long cables were modeled using 60 finite elements equally spaced. The initial configurations result from static equilibrium, considering gravity and buoyancy loads only. As depicted in Fig. 2, the cable of catenary shape, in a first analysis, will be tested for different periods of excitation of the platform movement. This movement is in the $0z$ direction with amplitude $U_0 = 2.5m$. The current profile is constant along the cable and with intensity of $0.8m/s$ in the Ox direction. For the periods of 20s and 15s of the oscillation movement of the platform, the deformed shapes of the cable are given in Fig. 4 and Fig. 5. These figures shows the large deformations assumed by the cable after a time of excitation of 100s.

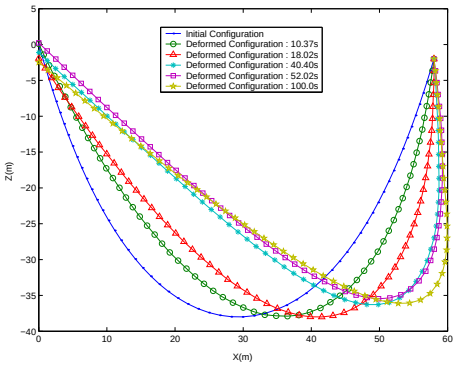

Figure 4. Deformed shapes for the period of 20s.

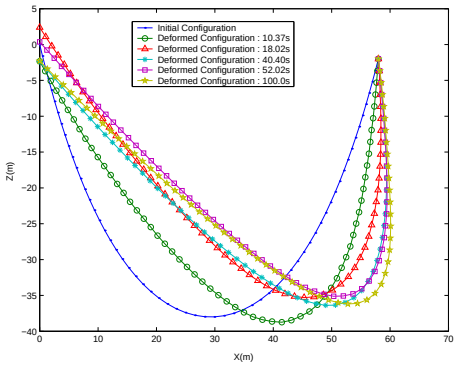

Figure 5. Deformed shapes for the period of 15s.

In a second analysis, a cable of initial catenary shape is tested for different intensities of the current profile. The platform movement in the $0z$ direction has period of 20s and amplitude $U_0 = 2.5m$. The current profiles are of $-0.1m/s$, $0m/s$, $0.25m/s$ and $0.50m/s$ and the deformed shapes are presented in Fig. 6, Fig. 7, Fig. 8 and Fig. 9 respectively. Once again it is emphasized that the numerical formulation can represent the nonlinear dynamics of the cable as depicted in Fig. 6, Fig. 8 and Fig. 9. Considering only the platform's motion, Fig. 7, the deformations are smaller when compared to the ones obtained when a current profile is assumed.

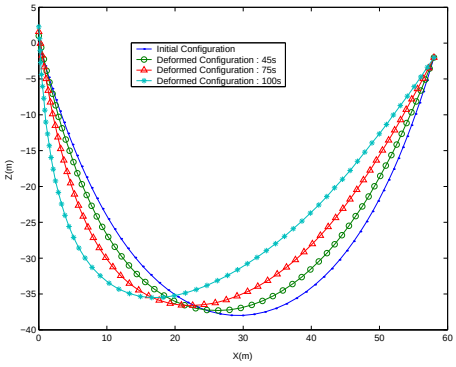

Figure 6. Deformed shapes - constant profile of -0.1m/s.

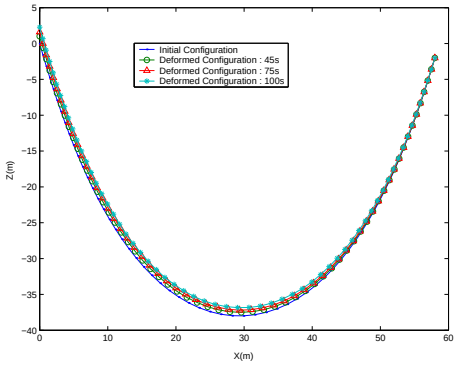

Figure 7. Deformed shapes - without current profile.

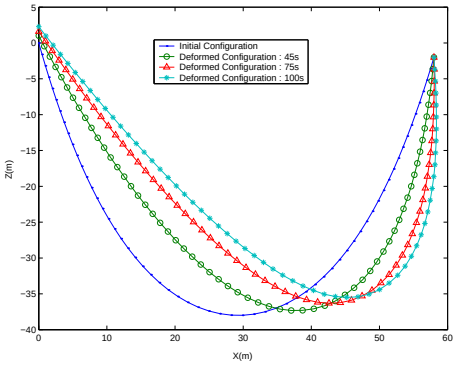

Figure 8. Deformed shapes - constant profile of 0.25m/s.

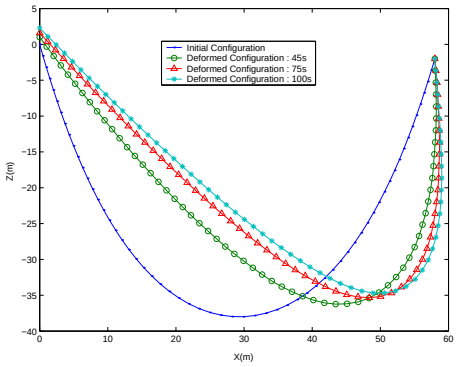

Figure 9. Deformed shapes - constant profile of 0.5m/s.

Figure 10 shows a sensitive study of the numerical formulation proposed for different finite element meshes of the cable. For the platform movement in the $0z$ direction with period of 20s and amplitude $U_0 = 2.5m$ and a current profile of $0.5m/s$ in the $0x$ direction, the deformed shapes are very similar for different finite element meshes of 10, 40, 54 and 60.

The central characteristic of the numerical formulation proposed here is the conservation of the total energy of the system for the Hamiltonian systems. Figure 11 shows the total mechanical energy of the system that is initially excited with the platform motion and after 15s of excitation has a free movement. As described by Fig. 11, the conservation of the total energy after this time of excitation is emphasized.

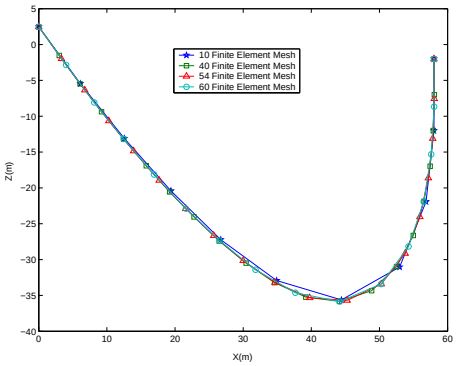

Figure 10. Deformed shapes - Comparison for different finite element meshes.

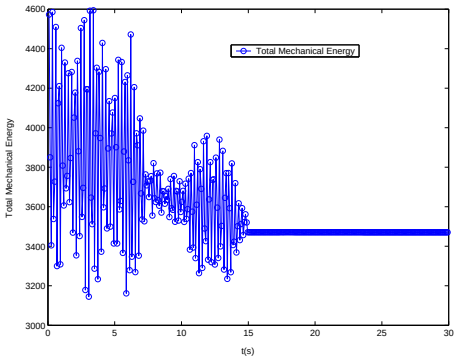

Figure 11. Total energy of the system

An alternative configuration with submerged buoys as depicted in Fig. 3 will now be tested. Suppose once again that a harmonic motion $U(t) = U_0 sin(wt)$ is imposed at the suspended end $S = 0$ in the $0z$ direction. This movement has a period of excitation of 30s and amplitude $U_0 = 2.5m$. The current profile varies linearly from 0.8m/s $(S = 0)$ to 0.3m/s $(S = l)$. It is important to notice that the submerged buoys load is of 0.67kN/m in the $0z$ direction. The cable initial configuration results from static equilibrium, considering gravity and buoyancy loads only. Figure 12 shows the cable lazy static equilibrium state and the deformed shapes due to the motion of the platform and the ocean current profile. A change of the current profile sign, produces the deformed shapes as depicted in Fig. 13.

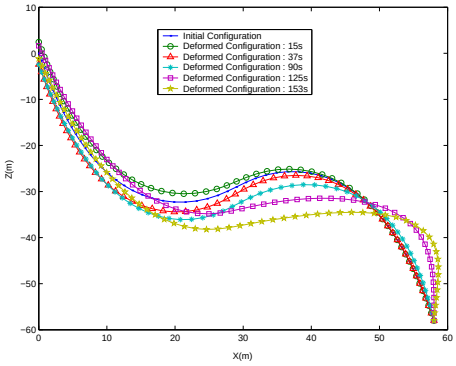

Figure 12. Deformed shapes.

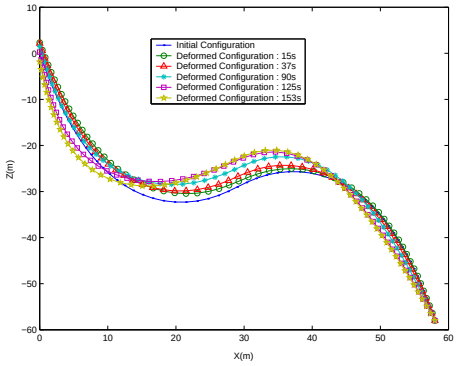

Figure 13. Deformed shapes for the reverse profile.

3. Final Remarks

In this work, a time stepping algorithm for the dynamic analysis of submarine cables has been presented. The solution procedure uses the variational formulation based on Hamilton's Principle to represent the cable dynamics and Lagrange multiplier technique to impose the cable deformation constraint of cross section rigid body motion. The solution results obtained using the algorithm in two samples (catenary and "lazy wave" cable configuration) has been presented to demonstrate the algorithm features.

4. References

Antman, S.S., Kenney, C.S., 1981, "Large Buckled States of Nonlinearly Elastic Rods under Torsion, Thrust and Gravity", Archieve of Rational Mechanics and Analysis, Vol.76, pp. 289-338.

Bailey, C.D., 1987, " Dynamics and the Calculus of Variations ", Computer Methods in Applied Mechanics and Engineering, Vol. 60, pp. 275-287.

Rochinha, F.A., 1990, "Modelling and Numerical Simulation of Rods", Phd Thesis-Puc Rio.

Dolinski, A., 1996, "Nonlinear Dynamics of Rods", Phd Thesis-UFRJ/COPPE Rio.

Geradin, M., 1994, "Application of the Finite Element Method to Dynamics of Articulated System", Internal Repport, University of Liègie.

Hughes, T.J.R., 1987, "The Finite Element Method", Prentice-Hall, New Jersey.

5. Responsibility notice

The authors are the only responsible for the printed material included in this paper.